# NUMERICAL IDENTIFICATION OF THE TIME-DEPENDENT COEFFICIENT IN THE HEAT EQUATION WITH FRACTIONAL LAPLACIAN

ARSHYN ALTYBAY, NIYAZ TOKMAGAMBETOV, AND GULZAT NALZHUPBAYEVA

ABSTRACT. We address the inverse problem of identifying a time-dependent source coefficient in a one-dimensional heat equation with a fractional Laplacian subject to Dirichlet boundary conditions and an integral nonlocal data. An a priori estimate is established to ensure the uniqueness and stability of the solution. A fully implicit Crank-Nicolson (CN) finite-difference scheme is proposed and rigorously analysed for stability and convergence. An efficient noise-stable computation algorithm is developed and verified through numerical experiments, demonstrating accuracy and robustness under noisy data.

### 1. Introduction

Let  $\Omega := (0, l) \subset \mathbb{R}$  be a bounded spatial interval and let T > 0 be a fixed final time. We consider the inverse problem of simultaneously determining a time-dependent coefficient r(t) and the corresponding state u(t, x) governed by the one-dimensional space-fractional heat equation

$$u_t(t,x) + (-\Delta)^s u(t,x) = r(t) f(t,x), \quad (t,x) \in Q := (0,T] \times \Omega,$$
 (1.1)

subject to the initial condition

$$u(0,x) = \varphi(x), \quad x \in \overline{\Omega},$$
 (1.2)

and homogeneous Dirichlet boundary conditions

$$u(t,0) = u(t,l) = 0, \quad t \in [0,T].$$
 (1.3)

The system is supplemented with the nonlocal integral overdetermination condition

$$\int_{\Omega} u(t,x)\,\omega(x)\,dx = w(t), \quad t \in [0,T],\tag{1.4}$$

which models spatially weighted internal measurements of the state.

Here u(t,x) denotes the state variable (e.g., temperature or concentration), and  $(-\Delta)^s$  is the one-dimensional fractional Laplace operator of order  $s \in (0,1)$  associated with homogeneous Dirichlet boundary conditions on  $\Omega$ . The source term satisfies  $f \in C^{1,2}(\overline{Q})$ , the initial datum is given by  $\varphi \in C^2(\overline{\Omega})$ , and  $r \in C[0,T]$  is the unknown time-dependent coefficient to be identified. The weight function  $\omega \in C^2([0,l])$  is a prescribed nonnegative function encoding the spatial sensitivity of the measurements, while  $w \in C^1([0,T])$  is a given measurement function.

Given the data  $\{f, \varphi, \omega, w\}$ , the inverse problem consists in reconstructing the pair  $\{r(t), u(t, x)\}$  on  $[0, T] \times \overline{\Omega}$ .

1

<sup>2020</sup> Mathematics Subject Classification. 65M06, 65M32, 35R30, 35B45.

Key words and phrases. inverse-coefficient problem, fractional heat equation, integral overdetermination condition, fractional Laplacian, numerical analysis.

The fractional Laplacian  $(-\Delta)^s$  models nonlocal diffusion by permitting longrange jumps with heavy-tailed step lengths; consequently, influence spreads instantaneously across the domain and the jump-length variance diverges-features typical of anomalous transport [1]. A central structural fact is that  $(-\Delta)^s$  is the infinitesimal generator of a symmetric  $\alpha$ -stable Lévy process with  $\alpha = 2s$ , which forges a direct bridge between PDE descriptions and stochastic path dynamics [2, 3, 4, 5, 6]. This probabilistic viewpoint explains the active study of both forward and inverse problems for nonlocal equations: parameters governing the jump process can be inferred from the data, while the PDE captures the macroscopic behaviour. The resulting framework underlies applications in quantitative finance [7, 8], nonlocal electromagnetic models [9], and flow through heterogeneous porous media [10], and it also accounts for anomalous diffusion in disordered physical systems [11] and empirically observed Lévy-flight foraging strategies in biology [12].

Numerous numerical methods have been developed for approximating the fractional Laplacian, including finite-difference schemes [13, 14, 15, 16, 17, 18, 19, 20], finite-element methods [21, 22, 23, 24, 25], spectral methods [26, 27, 28].

The integral overdetermination condition (1.4) represents a fundamental class of inverse problems where measurements correspond to spatially integrated quantities. This formulation was described in detail by Prilepko and his co-authors in their books published in 2000 [29]; it models practical scenarios where sensors capture aggregate field values rather than point measurements, such as total pollutant mass in environmental monitoring or integrated heat flux in thermal systems. The weighting function  $\omega(x)$  encodes the measurement device's spatial sensitivity, while w(t) provides the time-dependent global observation data essential for coefficient identification. Such integral overdetermination conditions have also been extensively investigated in the recent literature [30, 31, 32, 33, 34].

In recent years, the study of direct and inverse problems for fractional Laplacian operators has advanced markedly [35, 36, 37, 38, 39, 40, 41]. For instance, in [35], the authors established that, for both the classical heat equation and its space-time fractional counterpart, appropriately designed single measurements can determine key features of the underlying medium, thereby illustrating the power of nonlocal models in low-data inverse settings. In [36], the fractional Calderón problem was analysed, yielding global uniqueness and a constructive reconstruction scheme from a single measurement via Runge approximation and strong unique continuation. In [37], a multi-term space—time fractional diffusion model was considered, and the fractional orders themselves were shown to be simultaneously identifiable from suitable data. In [38], inverse problems for uncoupled space-time fractional operators with time-dependent coefficients were studied; the work developed an integrationby-parts framework for fractional-in-time derivatives and proved recovery of variable coefficients from exterior data. In [39], inverse problems for fractional equations with general nonlinearities were investigated, establishing well-posedness and global uniqueness results for recovering nonlinear potentials from boundary/exterior information. In [40], semilinear equations involving the fractional Laplacian were treated; the authors recovered the nonlinear term from a fractional Dirichlet-to-Neumann map by combining Runge-type approximation with unique continuation. Finally, in [41], inverse coefficient problems for the fractional heat equation were addressed, providing uniqueness and constructive identification strategies for timeand space-dependent coefficients from minimal data, including pointwise-in-time and nonlocal measurements.

Although these studies have substantially advanced the theoretical understanding of inverse problems-including those with the fractional Laplacian, limitations remain from a numerical-analysis standpoint: a comprehensive treatment of the full inverse problem, encompassing stability, convergence, and rigorous error estimation, as well as systematic testing under noisy data, is still lacking.

Because this work concerns inverse problems for the heat equation with a fractional Laplacian, we briefly review related studies in both time-fractional and classical parabolic settings. A substantial body of research addresses recovery of time-dependent coefficients under diverse boundary conditions and auxiliary data, including approaches based on integral overdetermination and nonlocal boundary conditions [42, 43, 44, 45].

This work fills a notable gap by delivering a robust numerical treatment of problems (1.1)–(1.4). We first derive an a priori estimate for the direct problem. We then devise a fully implicit, unconditionally stable finite-difference scheme and prove its stability and convergence. Finally, we present an efficient, noise-robust algorithm for the simultaneous identification of the pair  $\{r, u\}$ .

This paper is organised as follows. In Section 2, we introduce the key inequalities and foundational lemmas used throughout our analysis. Section 3 establishes the well-posedness results for both the direct and inverse problems. In Section 4, we describe a numerical method for the direct and inverse problem and provide its stability and convergence analysis. Finally, Section 5 presents and discusses the numerical experiments.

# 2. Preliminaries

In this section, we recall some fundamental definitions, inequalities, lemmas and theorems used throughout the paper.

**Definition 2.1** (Fractional Sobolev space). Given s > 0, the fractional Sobolev space is defined by

$$H^{s}(\mathbb{R}^{d}) = \big\{ f \in L^{2}(\mathbb{R}^{d}) : \int_{\mathbb{R}^{d}} (1 + |\xi|^{2s}) |\widehat{f}(\xi)|^{2} \, d\xi < +\infty \big\},$$

where  $\hat{f}$  denotes the Fourier transform of f.

We note that the fractional Sobolev space  $H^s$  endowed with the norm

$$||f||_{H^s} := \left( \int_{\mathbb{R}^d} (1+|\xi|^{2s}) |\widehat{f}(\xi)|^2 d\xi \right)^{\frac{1}{2}}, \text{ for } f \in H^s(\mathbb{R}^d),$$
 (2.1)

is a Hilbert space.

**Definition 2.2** (Fractional Laplacian). For s > 0,  $(-\Delta)^s$  denotes the fractional Laplacian defined by

$$(-\Delta)^s f = \mathcal{F}^{-1}(|\xi|^{2s}(\widehat{f})),$$

for all  $\xi \in \mathbb{R}^d$ .

In other words, the fractional Laplacian  $(-\Delta)^s$  can be viewed as the pseudo-differential operator with symbol  $|\xi|^{2s}$ . With this definition and the Plancherel theorem, the fractional Sobolev space can be defined as:

$$H^{s}(\mathbb{R}^{d}) = \left\{ f \in L^{2}(\mathbb{R}^{d}) : (-\Delta)^{\frac{s}{2}} f \in L^{2}(\mathbb{R}^{d}) \right\}, \tag{2.2}$$

moreover, the norm

$$||f||_{H^s} := ||f||_{L^2} + ||(-\Delta)^{\frac{s}{2}} f||_{L^2}, \tag{2.3}$$

is equivalent to the one defined in (2.1).

# **Definition 2.3.** A function

$$u \in C([0,T]; L^2(\Omega)) \cap C((0,T]; H_0^s(\Omega)) \cap C^1((0,T]; L^2(\Omega))$$

is called a weak solution of the problem  $\{(1.1), (1.2), (1.3)\}$  if it satisfies

$$(\partial_t u, v)_{L^2(\Omega)} + \langle u, v \rangle_{H_0^s(\mathbb{R}^n)} = (r(t)f, v)_{L^2(\Omega)}, \quad \forall v \in H_0^s(\Omega), \tag{2.4}$$

and the initial condition (1.2).

#### 3. Well-posedness of the direct and inverse problems

In this section, we show well-posedness of the direct and inverse problems defined by (1.1)–(1.4).

# 3.1. **Existence and Uniqueness Results.** We make the following assumptions for our problems:

- (1)  $r \in C([0,T])$ .
- (2)  $\varphi \in C^2([0,l])$  with  $\varphi(0) = \varphi(l) = 0$ .
- (3)  $f(t,x) \in C([0,T]; L^2(\Omega)) \cap C^1((0,T]; L^2(\Omega))$  and  $f(t,x) \neq 0$  for all  $t,x \in [0,T] \times \Omega$ .
- (4)  $\omega \in C^2([0, l])$  and  $\omega \neq 0 \ \forall t \in [0, T]$  and  $w \in C^1([0, T])$  with  $w(t) \neq 0$  for all  $t \in [0, T]$ .

The existence and uniqueness results of the inverse problem (1.1)-(1.4) have been theoretically established in [41] and read as follows.

**Lemma 3.1** (Existence and Uniqueness of Direct problem, e.g. Lemma 4 [41]). Let  $\varphi(x) \in L^2(\Omega)$  and  $f(t,x) \in C([0,T];L^2(\Omega)) \cap C^1((0,T];L^2(\Omega))$ . Then the function u(t,x) defined by (3.1) is a weak solution to Problem  $\{(1.1), (1.2), (1.3)\}$  for any  $r(t) \in C[0,T]$ .

$$u(t,x) = \sum_{k=1}^{\infty} \left( \varphi_k e^{-\lambda_k t} + \int_0^t f_k(\tau) e^{-\lambda_k (t-\tau)} r(\tau) d\tau \right) \varphi_k(x). \tag{3.1}$$

**Theorem 3.2** (Existence and Uniqueness of the Inverse Problem, e.g. Theorem 4 [41]). Let the assumptions of Lemma 3.1 and the following conditions hold:

- (1)  $\varphi \in D_m(\Omega)$ ;
- (2)  $f \in C(\Omega \times [0,T]), f(t,x) \in D_m(\Omega) \text{ and } \int_{\Omega} \omega(x) f(t,x) dx \neq 0 \text{ for all } t \in [0,T];$
- (3)  $w \in C^1[0,T]$  with  $w(t) \neq 0$  for all  $t \in [0,T]$  and  $w(0) = \int_{\Omega} \omega(x)\varphi(x) dx$ .

Here.

$$D_m(\Omega) = \begin{cases} \varphi : \varphi \in H_0^s(\Omega), & ((-\Delta)^s \varphi)^l \in H_0^s(\Omega), \ l = 0, \dots, m - 1; \\ and & ((-\Delta)^s \varphi)^m \in L^2(\Omega), \end{cases}$$

then, there exists a unique pair of functions (u, r) that solves Problems (1.1)–(1.4).

### 3.2. A priori estimate for the direct problem.

**Theorem 3.3** (A priori estimate). Let  $\Omega = (0, l)$ ,  $s \in (0, 1)$ ,  $r \in L^2(0, T)$ ,  $f \in L^2(0, T; L^2(\Omega))$ , and  $\varphi \in L^2(\Omega)$ . Then the solution u of (1.1)–(1.3) satisfies:

$$\|u(t,\cdot)\|_{L^{2}}^{2}+2\int_{0}^{t}\|(-\Delta)^{s/2}u(\tau,\cdot)\|_{L^{2}}^{2}d\tau \leq \left(\|\varphi(\cdot)\|_{L^{2}}^{2}+\frac{1}{\varepsilon}\int_{0}^{t}|r(\tau)|^{2}\|f(\tau,\cdot)\|_{L^{2}}^{2}d\tau\right)e^{\varepsilon t}.$$
(3.2)

for all  $t \in [0,T]$  and any  $\varepsilon > 0$ .

*Proof.* Multiply (1.1) by  $\overline{u}$  and integrate over (0,l), then take the real part:

$$Re\left(\left\langle u_t(t,\cdot),u(t,\cdot)\right\rangle_{L^2}+\left\langle (-\Delta)^s u(t,\cdot),u(t,\cdot)\right\rangle_{L^2}\right)=Re\left\langle r(t)f(t,\cdot),u(t,\cdot)\right\rangle_{L^2}.$$

We observe that:

$$Re\langle u_t(t,\cdot), u(t,\cdot)\rangle_{L^2} = \frac{1}{2} \frac{d}{dt} ||u(t,\cdot)||_{L^2}^2,$$

and by the self-adjointness and positivity of  $(-\Delta)^s$ .

$$Re\big\langle (-\Delta)^s u(t,\cdot), u(t,\cdot) \big\rangle_{L^2} = \|(-\Delta)^{s/2} u(t,\cdot)\|_{L^2}^2,$$

thus:

$$\frac{1}{2}\frac{d}{dt}\|u(t,\cdot)\|_{L^{2}}^{2}+\|(-\Delta)^{s/2}u(t,\cdot)\|_{L^{2}}^{2}=Re\big\langle r(t)f(t,\cdot),u(t,\cdot)\big\rangle_{L^{2}}.$$

Apply the Cauchy–Schwarz inequality and Young's inequality to the right-hand side:

$$Re\left\langle r(t)f(t,\cdot),u(t,\cdot)\right\rangle_{L^{2}}\leq\frac{\varepsilon}{2}\|u(t,\cdot)\|_{L^{2}}^{2}+\frac{|r(t)|^{2}}{2\varepsilon}\|f(t,\cdot)\|_{L^{2}}^{2}.$$

Hence:

$$\frac{1}{2}\frac{d}{dt}\|u(t,\cdot)\|_{L^2}^2 + \|(-\Delta)^{s/2}u(t,\cdot)\|_{L^2}^2 \leq \frac{\varepsilon}{2}\|u(t,\cdot)\|_{L^2}^2 + \frac{|r(t)|^2}{2\varepsilon}\|f(t,\cdot)\|_{L^2}^2.$$

Multiplying by 2 and integrating over time, we get

$$\|u(t,\cdot)\|_{L^{2}}^{2}+2\int_{0}^{t}\|(-\Delta)^{s/2}u(\tau,\cdot)\|_{L^{2}}^{2}d\tau \leq \|\varphi(\cdot)\|_{L^{2}}^{2}+\varepsilon\int_{0}^{t}\|u(\tau,\cdot)\|_{L^{2}}^{2}d\tau+\frac{1}{\varepsilon}\int_{0}^{t}|r(\tau)|^{2}\|f(\tau,\cdot)\|_{L^{2}}^{2}d\tau.$$
(3.3)

Define the total energy:

$$E(t) = \|u(t, \cdot)\|_{L^2}^2 + 2 \int_0^t \|(-\Delta)^{s/2} u(\tau, \cdot)\|_{L^2}^2 d\tau.$$

Note that  $||u(\tau,\cdot)||_{L^2}^2 \leq E(\tau)$  for all  $\tau \in [0,t]$  (because the dissipation term is nonnegative), inequality (3.3) becomes:

$$E(t) \le \|\varphi(\cdot)\|_{L^{2}}^{2} + \varepsilon \int_{0}^{t} E(\tau)d\tau + \frac{1}{\varepsilon} \int_{0}^{t} |r(\tau)|^{2} \|f(\tau, \cdot)\|_{L^{2}}^{2} d\tau.$$
 (3.4)

Applying Gronwall's inequality to (3.4) yields:

$$E(t) \le \left( \|\varphi(\cdot)\|_{L^2}^2 + \frac{1}{\varepsilon} \int_0^t |r(\tau)|^2 \|f(\tau, \cdot)\|_{L^2}^2 d\tau \right) e^{\varepsilon t}.$$

Substituting back the definition of E(t) yields the desired estimate (3.2).

The a priori estimate (3.2) also ensures both the uniqueness and continuous dependence of the solution to problem (1.1)-(1.3) on the initial data.

In the remainder of this work, we focus on the numerical solution of the inverse problem (1.1)-(1.4). Building upon the established existence and uniqueness results, we develop and implement stable numerical schemes to approximate both the state variable u(x,t) and the unknown time-dependent coefficient r(t). Our goal is to construct stable and accurate numerical method that efficiently identifies the inverse data from available measurements.

#### 4. Numerical solution of the direct and inverse problems

In this section, we present a numerical solution to the Direct and Inverse problems for the fractional diffusion equation (1.1) with initial condition (1.2) and boundary conditions (1.3), using the integral measurement (1.3), and employing the finite difference method.

4.1. The implicit finite difference schemes for the direct problem. In this subsection, we present a numerical solution of the direct problem for the heat equation (1.1) with initial (1.2) and boundary (1.3) using the finite difference method. Let  $\Omega = (0, l), 0 < s < 1, T > 0$ . For any  $u : \mathbb{R} \to \mathbb{R}$  extended by zero outside (0,l), the Riesz fractional Laplacian is defined by

$$(-\Delta)^{s} u(x) = c_{1,s} \text{ p.v.} \int_{\mathbb{R}} \frac{u(x) - u(y)}{|x - y|^{1 + 2s}} \, dy, \qquad c_{1,s} = \frac{4^{s} s \, \Gamma(\frac{1}{2} + s)}{\sqrt{\pi} \, |\Gamma(1 - s)|}. \tag{4.1}$$

with  $u \equiv 0$  on  $\mathbb{R} \setminus (0, l)$  and the "p.v." denotes the principal value of the integral and the  $c_{1,s}$  is the normalization constant.

We divide the spatial domain [0, l] into N grid points with spacing h = l/N time domain [0,T] into M grid points with spacing  $\tau = T/M$ . Let the grid points be denoted as  $x_i = ih$ , i = 0, 1, ..., N,  $t_n = n\tau$ , for n = 0, 1, ..., M. Let  $u_i^n$  be the numerical approximation to  $u(t_n, x_i, )$ .

Using the zero exterior extension  $u \equiv 0$  on  $\mathbb{R} \setminus (0, l)$ , the operator (4.1) can be

$$(-\Delta)^s u(x_i) = c_{1,s} \left( \text{p.v.} \int_0^l \frac{u(x_i) - u(y)}{|x_i - y|^{1+2s}} \, dy + u(x_i) \int_{\mathbb{R} \setminus \{0,l\}} \frac{1}{|x_i - y|^{1+2s}} \, dy \right).$$

The interior integral is approximated by the midpoint quadrature on the mesh:

p.v. 
$$\int_0^l \frac{u(x_i) - u(y)}{|x_i - y|^{1+2s}} dy \approx h \sum_{\substack{j=1\\j \neq i}}^{N-1} \frac{u_i - u_j}{|x_i - x_j|^{1+2s}}.$$

The exterior contribution admits the closed form 
$$\int_{\mathbb{R}\backslash\{0,l\}}\frac{1}{|x_i-y|^{1+2s}}\,dy=\frac{1}{2s}\left(x_i^{-2s}+(l-x_i)^{-2s}\right),\qquad x_i=ih.$$

Thus, the fully discrete operator can be written as

$$(A\mathbf{U})_i = c_{1,s} \left[ h \sum_{\substack{j=1\\j\neq i}}^{N-1} \frac{u_i - u_j}{|x_i - x_j|^{1+2s}} + u_i \frac{1}{2s} \left( x_i^{-2s} + (l - x_i)^{-2s} \right) \right], \qquad i = 1, \dots, N-1,$$

here,  $\mathbf{U} = (u_1, \dots, u_{N-1})^{\top}$ .

Using  $|x_i-x_j|=h|i-j|$ , the entries of the *dense* stiffness matrix  $A \in \mathbb{R}^{(N-1)\times(N-1)}$  take the explicit form:

Off-diagonal entries  $(i \neq j)$ :

$$A_{ij} = -\frac{c_{1,s}}{h^{2s}} \frac{1}{|i-j|^{1+2s}}, \qquad 1 \le i \ne j \le N-1.$$
(4.2)

Diagonal entries:

$$A_{ii} = \frac{c_{1,s}}{h^{2s}} \left[ \sum_{\substack{j=1\\j\neq i}}^{N-1} \frac{1}{|i-j|^{1+2s}} + \frac{1}{2s} (i^{-2s} + (N-i)^{-2s}) \right], \qquad i = 1, \dots, N-1.$$
(4.3)

The matrix A is symmetric, strictly positive definite, and fully dense. The non-Toeplitz structure of the diagonal entries reflects the strong dependence of the Dirichlet fractional Laplacian on the distance to the boundary.

We use the Crank-Nicolson based scheme then problem (1.1)-(1.3) and it can be rewritten in the following form:

$$\frac{u_i^{n+1} - u_i^n}{\tau} + \frac{1}{2}((-\Delta)^s u_i^{n+1} + (-\Delta)^s u_i^n) = r^{n+1/2} f_i^{n+1/2},\tag{4.4}$$

where  $r^{n+\frac{1}{2}} \in \mathbb{R}$  and  $f^{n+\frac{1}{2}} \in \mathbb{R}$  are the given midpoint coefficients and forcing vectors, respectively.

The initial condition is discretised as:

$$u_i^0 = \varphi(x_i), \tag{4.5}$$

with homogeneous Dirichlet data

$$u_0^n = 0, \ u_N^n = 0. (4.6)$$

Substituting the matrix approximation  $(-\Delta)^s \mathbf{U} \approx A\mathbf{U}$ , we get:

$$\frac{\mathbf{U}^{n+1} - \mathbf{U}^n}{\tau} + \frac{1}{2}(A\mathbf{U}^{n+1} + A\mathbf{U}^n) = r^{n+1/2}\mathbf{F}^{n+1/2}.$$
 (4.7)

Rearranging terms:

$$(I + \frac{\tau}{2} A) \mathbf{U}^{n+1} = (I - \frac{\tau}{2} A) \mathbf{U}^n + \tau r^{n+1/2} \mathbf{F}^{n+\frac{1}{2}},$$
 (4.8)

where

$$\mathbf{U}^{n} = \left(u_{1}^{n}, \dots, u_{N-1}^{n}\right)^{\top}, \qquad \mathbf{F}^{n+\frac{1}{2}} = \left(f(x_{1}, t^{n+\frac{1}{2}}), \dots, f(x_{N-1}, t^{n+\frac{1}{2}})\right)^{\top}.$$

**Remark 4.1.** A is symmetric positive definite; hence the left-hand matrix  $P := I + \frac{\tau}{2}A$  in (4.8) is SPD, and one can solve (4.8) efficiently with Conjugate Gradient (CG) method or Preconditioned Conjugate Gradient (PCG) method.

4.2. Stability of the implicit difference schemes. To justify the proposed algorithm, we will derive estimates of the stability of schemes (4.4) - (4.6) concerning the initial data and the right-hand side.

**Theorem 4.2** (Stability). Consider the Crank–Nicolson (CN) scheme (4.7). Define the midpoint state  $\mathbf{U}^{n+\frac{1}{2}} := \frac{1}{2}(\mathbf{U}^{n+1} + \mathbf{U}^n)$ . Then the following hold, for any  $\tau > 0$  (i.e., unconditionally):

(i) Homogeneous case  $(\mathbf{F}^{n+\frac{1}{2}} \equiv \mathbf{0})$ . One has the exact energy identity

$$\|\mathbf{U}^{n+1}\|_{L^{2}}^{2} + 2\tau \|\mathbf{U}^{n+\frac{1}{2}}\|_{A}^{2} = \|\mathbf{U}^{n}\|_{L^{2}}^{2}, \tag{4.9}$$

and, in particular,  $\|\mathbf{U}^{n+1}\|_{L^2} \leq \|\mathbf{U}^n\|_{L^2}$  for all n.

(ii)  $L^2$ -stability with forcing. For arbitrary data  $r^{n+\frac{1}{2}}$  and  $\mathbf{F}^{n+\frac{1}{2}}$ ,

$$\|\mathbf{U}^n\|_{L^2} \le \|\mathbf{U}^0\|_{L^2} + \sum_{k=0}^{n-1} \tau |r^{k+\frac{1}{2}}| \|\mathbf{F}^{k+\frac{1}{2}}\|_{L^2}, \quad n = 1, \dots, M.$$
 (4.10)

(iii) Energy estimate with dissipation. For arbitrary data  $r^{n+\frac{1}{2}}$  and  $\mathbf{F}^{n+\frac{1}{2}}$ ,

$$\|\mathbf{U}^{n}\|_{L^{2}}^{2} + \sum_{k=0}^{n-1} \tau \|\mathbf{U}^{k+\frac{1}{2}}\|_{A}^{2} \leq \|\mathbf{U}^{0}\|_{L^{2}}^{2} + \sum_{k=0}^{n-1} \tau |r^{k+\frac{1}{2}}|^{2} \|\mathbf{F}^{k+\frac{1}{2}}\|_{A^{-1}}^{2}, \qquad n = 1, \dots, M,$$
(4.11)

where  $\|\cdot\|_{L^2}$  denotes the Euclidean norm on  $\mathbb{R}^{N-1}$ ,  $\|v\|_A^2 := \langle Av, v \rangle$  is the energy norm (since A is SPD), and  $\|v\|_{A^{-1}}^2 := \langle A^{-1}v, v \rangle$  is the corresponding dual norm. Consequently, the CN scheme (4.7) is unconditionally stable in both  $L^2$  and the energy sense.

*Proof.* We work directly with the CN form (4.7). Taking the Euclidean inner product of (4.7) with  $\mathbf{U}^{n+1} + \mathbf{U}^n$  and using the symmetry of A yields

$$\frac{1}{\tau} \left\langle \mathbf{U}^{n+1} - \mathbf{U}^{n}, \ \mathbf{U}^{n+1} + \mathbf{U}^{n} \right\rangle + \frac{1}{2} \left\langle A(\mathbf{U}^{n+1} + \mathbf{U}^{n}), \ \mathbf{U}^{n+1} + \mathbf{U}^{n} \right\rangle = r^{n+\frac{1}{2}} \left\langle \mathbf{F}^{n+\frac{1}{2}}, \ \mathbf{U}^{n+1} + \mathbf{U}^{n} \right\rangle. \tag{4.12}$$

Observe that

$$\left< \mathbf{U}^{n+1} - \mathbf{U}^n, \ \mathbf{U}^{n+1} + \mathbf{U}^n \right> = \|\mathbf{U}^{n+1}\|_{L^2}^2 - \|\mathbf{U}^n\|_{L^2}^2,$$

and, with  $\mathbf{U}^{n+\frac{1}{2}} := \frac{1}{2}(\mathbf{U}^{n+1} + \mathbf{U}^n),$ 

$$\frac{1}{2} \langle A(\mathbf{U}^{n+1} + \mathbf{U}^n), \, \mathbf{U}^{n+1} + \mathbf{U}^n \rangle = 2 \| \mathbf{U}^{n+\frac{1}{2}} \|_A^2.$$

Thus (4.12) becomes the basic energy identity

$$\frac{\|\mathbf{U}^{n+1}\|_{L^{2}}^{2} - \|\mathbf{U}^{n}\|_{L^{2}}^{2}}{\tau} + 2\|\mathbf{U}^{n+\frac{1}{2}}\|_{A}^{2} = 2r^{n+\frac{1}{2}} \langle \mathbf{F}^{n+\frac{1}{2}}, \mathbf{U}^{n+\frac{1}{2}} \rangle. \tag{4.13}$$

(i) Homogeneous case. If  $\mathbf{F}^{n+\frac{1}{2}} \equiv \mathbf{0}$ , the right-hand side of (4.13) vanishes and we obtain

$$\|\mathbf{U}^{n+1}\|_{L^2}^2 + 2\tau \|\mathbf{U}^{n+\frac{1}{2}}\|_A^2 = \|\mathbf{U}^n\|_{L^2}^2,$$

which is (4.9). In particular,  $\|\mathbf{U}^{n+1}\|_{L^2} \leq \|\mathbf{U}^n\|_{L^2}$ .

(ii)  $L^2$ -stability with forcing. From (4.13), drop the nonnegative term  $2 \|\mathbf{U}^{n+\frac{1}{2}}\|_A^2$  and apply Cauchy–Schwarz:

$$\frac{\|\mathbf{U}^{n+1}\|_{L^{2}}^{2} - \|\mathbf{U}^{n}\|_{L^{2}}^{2}}{\tau} \leq 2 |r^{n+\frac{1}{2}}| \|\mathbf{F}^{n+\frac{1}{2}}\|_{L^{2}} \|\mathbf{U}^{n+\frac{1}{2}}\|_{L^{2}} \leq |r^{n+\frac{1}{2}}| \|\mathbf{F}^{n+\frac{1}{2}}\|_{L^{2}} (\|\mathbf{U}^{n+1}\|_{L^{2}} + \|\mathbf{U}^{n}\|_{L^{2}}).$$

Using  $a^2 - b^2 = (a - b)(a + b)$  with  $a = \|\mathbf{U}^{n+1}\|, b = \|\mathbf{U}^n\|$ , we obtain

$$\frac{\|\mathbf{U}^{n+1}\|_{L^2} - \|\mathbf{U}^n\|_{L^2}}{\tau} \le |r^{n+\frac{1}{2}}| \|\mathbf{F}^{n+\frac{1}{2}}\|_{L^2}.$$

Summing over n = 0, ..., m-1 yields (4.10) with n = m.

(iii) Energy estimate with dissipation. Since A is symmetric positive definite, the dual norm  $\|\mathbf{F}^{n+\frac{1}{2}}\|_{A^{-1}}$  is well-defined via the identity:

$$\|\mathbf{F}^{n+\frac{1}{2}}\|_{A^{-1}} = \sup_{\mathbf{V} \neq 0} \frac{\|\left\langle \mathbf{F}^{n+\frac{1}{2}}, \mathbf{V} \right\rangle\|}{\|\mathbf{V}\|_{A}}.$$

From (4.13), apply the dual Cauchy–Schwarz inequality

$$\left| \left< \mathbf{F}^{\, n + \frac{1}{2}}, \, \mathbf{U}^{n + \frac{1}{2}} \right> \right| \leq \| \mathbf{U}^{n + \frac{1}{2}} \|_A \, \| \mathbf{F}^{\, n + \frac{1}{2}} \|_{A^{-1}},$$

and then Young's inequality with  $\varepsilon = 1$ :

$$2\,|r^{\,n+\frac{1}{2}}|\,\|\mathbf{U}^{n+\frac{1}{2}}\|_A\,\|\mathbf{F}^{\,n+\frac{1}{2}}\|_{A^{-1}}\,\,\leq\,\,\|\mathbf{U}^{n+\frac{1}{2}}\|_A^2\,\,+\,\,|r^{\,n+\frac{1}{2}}|^2\,\|\mathbf{F}^{\,n+\frac{1}{2}}\|_{A^{-1}}^2.$$

Therefore,

$$\frac{\|\mathbf{U}^{n+1}\|^2 - \|\mathbf{U}^n\|^2}{\tau} + \|\mathbf{U}^{n+\frac{1}{2}}\|_A^2 \le |r^{n+\frac{1}{2}}|^2 \|\mathbf{F}^{n+\frac{1}{2}}\|_{A^{-1}}^2.$$

Summing in n = 0, ..., m - 1 gives (4.11) with n = m.

- **Remark 4.3** (Modal view and A-stability). Since A is SPD, there exists an orthonormal basis of eigenvectors with positive eigenvalues  $\lambda > 0$ . On each mode the homogeneous CN update reads  $\widehat{U}^{n+1} = g(\mu)\widehat{U}^n$  with  $g(\mu) = (1 \mu/2)/(1 + \mu/2)$  and  $\mu = \tau \lambda \geq 0$ , hence  $|g(\mu)| \leq 1$  for all  $\mu \geq 0$ . This confirms A-stability and contractivity of CN on the fractional heat operator.
- 4.3. Convergence analysis. Building upon the unconditional stability in Theorem 4.2, we now establish the convergence of the Crank–Nicolson scheme (4.8) when the fractional Laplacian  $(-\Delta)^s$  is discretised by the dense Dirichlet stiffness matrix A defined in (4.2)–(4.3).
- **Lemma 4.4** (Consistency of the dense Dirichlet fractional Laplacian). Let  $s \in (0,1)$  and  $u(\cdot) \in H^{s+2}(\Omega)$  be extended by zero outside (0,l). Let  $\mathbf{u} = (u(x_1), \dots, u(x_{N-1}))^{\top}$  be the nodal samples at  $x_i = ih$ , and let A be the dense Dirichlet matrix defined by (4.2)-(4.3). Then there exists a constant C > 0, independent of h and  $\tau$ , such that

$$\left\| A \mathbf{u} - \left( (-\Delta)^s u \right) \right|_{\{x_i\}} \right\|_{L^2} \le C h^{2-2s} \|u\|_{H^{s+2}(\Omega)}. \tag{4.14}$$

If  $u(\cdot,t) \in H^{s+2}(\Omega)$  uniformly in  $t \in [0,T]$ , then the bound holds uniformly in t.

*Proof (sketch)*. Recall the integral representation of the Dirichlet fractional Laplacian

$$(-\Delta)^{s} u(x_{i}) = c_{1,s} \text{ p.v.} \int_{0}^{l} \frac{u(x_{i}) - u(y)}{|x_{i} - y|^{1+2s}} \, dy + c_{1,s} \, u(x_{i}) \int_{\mathbb{R} \setminus \{0,l\}} \frac{1}{|x_{i} - y|^{1+2s}} \, dy,$$

with zero exterior extension. In A the exterior integral is evaluated exactly, while the interior principal value integral is approximated by a midpoint quadrature on the uniform grid:

$$\int_0^l \frac{u(x_i) - u(y)}{|x_i - y|^{1+2s}} \, dy \approx h \sum_{\substack{j=1\\ i \neq i}}^{N-1} \frac{u(x_i) - u(x_j)}{|x_i - x_j|^{1+2s}}.$$

The quadrature error can be split into a near-field part (in a neighbourhood of  $y = x_i$ ) and a far-field part. For the far field, where  $|x_i - y| \ge ch$ , the integrand

is smooth and the midpoint rule yields an  $O(h^2)$  error. In the near field, using a Taylor expansion of u around  $x_i$ ,

$$u(x_i) - u(y) = \frac{1}{2}u''(x_i)(x_i - y)^2 + O(|x_i - y|^3),$$

and thus the local integrand behaves like  $|x_i - y|^{1-2s}$ . Integrating over an interval of width O(h) around  $x_i$  gives a contribution of order  $h^{2-2s}$ . This term dominates the  $O(h^2)$  far-field contribution, and therefore

$$\left| (-\Delta)^s u(x_i) - (A\mathbf{u})_i \right| \le C h^{2-2s} \|u\|_{H^{s+2}(\Omega)}.$$

Summing over i and using the equivalence between the discrete  $L^2$  norm and the continuous  $L^2$  norm on the grid, we obtain (4.14). A rigorous version of this argument is in line with the truncation error analysis for one-dimensional integral fractional Laplacian discretisations, see for instance [17], where the rate  $O(h^{2-\alpha})$  is established for order- $\alpha$  operators; identifying  $\alpha = 2s$  yields  $O(h^{2-2s})$ .

**Theorem 4.5** (Convergence). Assume the hypotheses of Theorem 4.2 and Lemma 4.4, exact midpoint data  $r^{n+\frac{1}{2}}$ ,  $\mathbf{F}^{n+\frac{1}{2}}$ , and exact nodal initialisation  $\mathbf{U}^0 = \mathbf{u}^0$ . Then the Crank–Nicolson solution  $\mathbf{U}^n$  of (4.8) with A satisfies

$$\max_{0 \le n \le M} \|\mathbf{u}^n - \mathbf{U}^n\|_A \le C \left(\tau^2 + h^{2-2s}\right), \tag{4.15}$$

with a constant C > 0 independent of h and  $\tau$ .

*Proof.* Define the error  $\mathbf{e}^n := \mathbf{u}^n - \mathbf{U}^n$  and the midpoint  $\mathbf{e}^{n+\frac{1}{2}} := \frac{1}{2}(\mathbf{e}^{n+1} + \mathbf{e}^n)$ . Subtracting the discrete scheme for  $\mathbf{U}^n$  from the scheme satisfied by the exact nodal values  $\mathbf{u}^n$  (obtained by inserting the PDE at  $t^{n+\frac{1}{2}}$  and replacing  $(-\Delta)^s$  by A) yields

$$\frac{\mathbf{e}^{n+1} - \mathbf{e}^n}{\tau} + \frac{1}{2} A(\mathbf{e}^{n+1} + \mathbf{e}^n) = \boldsymbol{\xi}^{n+\frac{1}{2}}, \tag{4.16}$$

where the local defect is

$$\boldsymbol{\xi}^{n+\frac{1}{2}} := \underbrace{\frac{\mathbf{u}^{n+1} - \mathbf{u}^n}{\tau} - \left(u_t(\cdot, t^{n+\frac{1}{2}})\right)\big|_{\{x_i\}}}_{\text{time discretisation error}} + \underbrace{A\,\mathbf{u}^{n+\frac{1}{2}} - \left((-\Delta)^s u(\cdot, t^{n+\frac{1}{2}})\right)\big|_{\{x_i\}}}_{\text{space discretisation error}}.$$

By Taylor expansion in time, the CN scheme is second-order accurate, hence

$$\left\| \frac{\mathbf{u}^{n+1} - \mathbf{u}^n}{\tau} - u_t(\cdot, t^{n+\frac{1}{2}}) \right|_{\{x_i\}} \right\|_{L^2} \leq C \tau^2.$$

By Lemma 4.4, the spatial defect satisfies

$$||A\mathbf{u}^{n+\frac{1}{2}} - (-\Delta)^s u(\cdot, t^{n+\frac{1}{2}})|_{\{x_i\}}||_{L^2} \le C h^{2-2s}.$$

Combining both estimates,

$$\|\boldsymbol{\xi}^{n+\frac{1}{2}}\|_{L^2} \le C(\tau^2 + h^{2-2s}), \qquad 0 \le n \le M-1.$$
 (4.17)

Equation (4.16) is the Crank–Nicolson scheme with homogeneous data and a forcing term  $\boldsymbol{\xi}^{n+\frac{1}{2}}$ . Applying the  $L^2$ -stability estimate (4.10) of Theorem 4.2 to (4.16), and using  $\mathbf{e}^0 = \mathbf{0}$ , we obtain

$$\|\mathbf{e}^n\|_{L^2} \le \sum_{k=0}^{n-1} \tau \|\boldsymbol{\xi}^{k+\frac{1}{2}}\|_{L^2} \le CT(\tau^2 + h^{2-2s}).$$

Taking the maximum over n and using the equivalence between the discrete  $L^2$  norm and the discrete energy norm on the interior grid yields (4.15). This completes the proof.

4.4. Numerical algorithm for solving the Inverse Problem. This subsection presents a numerical method for simultaneously identifying the time-dependent coefficient r(t) and computing the solution u(t, x) of the inverse problem (1.1)-(1.4).

We first consider a classical approach that leverages the overdetermination condition (1.4) to derive an explicit formula for the unknown coefficient r(t), assuming that the solution u(t,x) is available at each time step via numerical simulation of the direct problem (1.1)–(1.3). We rewrite our full CN scheme for the direct problem again

$$(I + \frac{\tau}{2} A) \mathbf{U}^{n+1} = (I - \frac{\tau}{2} A) \mathbf{U}^n + \tau r^{n+\frac{1}{2}} \mathbf{F}^{n+\frac{1}{2}},$$

where  $U^n \in \mathbb{R}^{N-1}$  collects the nodal values  $u(t^n, x_i)$  at the interior grid points and A is the SPD stiffness matrix approximating the Dirichlet fractional Laplacian. Introduce the time-stepping operators

$$L := I + \frac{\tau}{2}A, \qquad R := I - \frac{\tau}{2}A.$$

Then the CN update can be written as

$$L \mathbf{U}^{n+1} = R \mathbf{U}^n + \tau r^{n+\frac{1}{2}} \mathbf{F}^{n+\frac{1}{2}}. \tag{4.18}$$

Solve once with L for the two right-hand sides:

$$\mathbf{Y} := L^{-1}R\mathbf{U}^n, \qquad \mathbf{S} := L^{-1}\mathbf{F}^{n+\frac{1}{2}}.$$
 (4.19)

Then (4.18) gives the explicit representation

$$\mathbf{U}^{n+1} = \mathbf{Y} + \tau r^{n+\frac{1}{2}} \mathbf{S}. \tag{4.20}$$

The discrete counterpart of the integral identity  $\frac{d}{dt} \int u \, \omega = -\int (-\Delta)^s u \, \omega + r \int f \, \omega$  evaluated at the midpoint  $t^{n+\frac{1}{2}}$  is

$$\frac{w^{n+1}-w^n}{\tau} \ = \ -h \left\langle A \, \mathbf{U}^{\mathrm{avg}}, \, \boldsymbol{\omega} \right\rangle \ + \ r^{n+\frac{1}{2}} \, h \left\langle \mathbf{F}^{\, n+\frac{1}{2}}, \, \boldsymbol{\omega} \right\rangle, \qquad \mathbf{U}^{\mathrm{avg}} := \frac{\mathbf{U}^{n+1} + \mathbf{U}^n}{2}. \tag{4.21}$$

Here  $w^n = w(t^n)$  are the measured integrals. The difficulty is that  $\mathbf{U}^{\text{avg}}$  contains  $\mathbf{U}^{n+1}$ , which itself depends on  $r^{n+\frac{1}{2}}$ . We therefore eliminate  $\mathbf{U}^{n+1}$  using (4.20).

$$U^{avg} := \frac{1}{2}(U^{n+1} + U^n).$$

Splitting  $U^{avg}$  into a known part plus a part linear in r. Define the midpoint split

$$\mathbf{V} := \frac{\mathbf{U}^n + \mathbf{Y}}{2}.\tag{4.22}$$

Using (4.20), we obtain

$$\mathbf{U}^{\text{avg}} = \frac{\mathbf{U}^n + \mathbf{U}^{n+1}}{2} = \frac{\mathbf{U}^n + \mathbf{Y}}{2} + \frac{\tau}{2} \, r^{n + \frac{1}{2}} \, \mathbf{S} = \mathbf{V} + \frac{\tau}{2} \, r^{n + \frac{1}{2}} \, \mathbf{S}.$$

Applying A and pairing with  $\omega$  yields

$$h \langle A \mathbf{U}^{\text{avg}}, \boldsymbol{\omega} \rangle = h \langle A \mathbf{V}, \boldsymbol{\omega} \rangle + \frac{\tau}{2} r^{n + \frac{1}{2}} h \langle A \mathbf{S}, \boldsymbol{\omega} \rangle.$$
 (4.23)

Substituting (4.23) into (4.21) and rearranging terms in  $r^{n+\frac{1}{2}}$ , we obtain

$$\frac{w^{n+1}-w^n}{\tau} = -\left(h\left\langle A\,\mathbf{V},\,\boldsymbol{\omega}\right\rangle + \frac{\tau}{2}\,r^{n+\frac{1}{2}}\,h\left\langle A\,\mathbf{S},\,\boldsymbol{\omega}\right\rangle\right) + r^{n+\frac{1}{2}}\,h\left\langle \mathbf{F}^{\,n+\frac{1}{2}},\,\boldsymbol{\omega}\right\rangle,$$

and hence

$$\frac{w^{n+1}-w^n}{\tau}+h\left\langle A\,\mathbf{V},\,\boldsymbol{\omega}\right\rangle =r^{n+\frac{1}{2}}\left(h\left\langle \mathbf{F}^{\,n+\frac{1}{2}},\,\boldsymbol{\omega}\right\rangle -\frac{\tau}{2}\,h\left\langle A\,\mathbf{S},\,\boldsymbol{\omega}\right\rangle \right)\!.$$

Assuming that the denominator does not vanish, we arrive at the closed expression

$$r^{n+\frac{1}{2}} = \frac{\frac{w^{n+1} - w^n}{\tau} + h \langle A\mathbf{V}, \boldsymbol{\omega} \rangle}{h \langle \mathbf{F}^{n+\frac{1}{2}}, \boldsymbol{\omega} \rangle - \frac{\tau}{2} h \langle A\mathbf{S}, \boldsymbol{\omega} \rangle}.$$
 (4.24)

The full computational procedure is summarised in Algorithm 1.

**Algorithm 1** CN-Riesz algorithm for simultaneous recovery  $\{r(t), u(t, x)\}$ 

**Require:** Grid:  $x_i = ih$ , i = 0, ..., N,  $t^n = n\tau$ , n = 0, ..., M. Interior indices i = 1, ..., N - 1.

**Require:** Data: initial  $\varphi(x)$ , forcing f(t,x), weight  $\omega(x)$ , measured integrals w(t). **Require:** SPD Riesz matrix A on interior nodes.

- 1: **Initialization.** Set  $\mathbf{U}^0 = (\varphi(x_1), \dots, \varphi(x_{N-1}))^{\top}$ . Build the vectors  $\boldsymbol{\omega} = (\omega(x_1), \dots, \omega(x_{N-1}))^{\top}$ .
- 2: Time-stepping operators. Let

$$L:=I+\tfrac{\tau}{2}A, \qquad R:=I-\tfrac{\tau}{2}A.$$

- 3: **for** n = 0 **to** M 1 **do**
- 4: Midpoint forcing. Assemble  $\mathbf{F}^{n+\frac{1}{2}} = (f(x_i, t^{n+\frac{1}{2}}))_{i=1}^{N-1}$ .
- 5: Two solves with the same SPD matrix L.

$$\mathbf{Y} := L^{-1}R\mathbf{U}^n, \quad \mathbf{S} := L^{-1}\mathbf{F}^{n+\frac{1}{2}}.$$

6: Midpoint state split. Set  $V := \frac{1}{2}(U^n + Y)$ . Then

$$\frac{1}{2}(\mathbf{U}^{n+1} + \mathbf{U}^n) = \mathbf{V} + \frac{\tau}{2} r^{n+\frac{1}{2}} \mathbf{S}.$$

- 7: Recover  $r^{n+\frac{1}{2}}$  using the formula (4.24)
- 8: Update  $U^{n+1}$

$$\mathbf{U}^{n+1} = \mathbf{Y} + \tau r^{n+\frac{1}{2}} \mathbf{S}.$$

- 9: end for
- 10: **return**  $\{\mathbf{U}^n\}_{n=0}^M$  (hence  $u(t^n, x_i)$ ) and  $\{r^{n+\frac{1}{2}}\}_{n=0}^{M-1}$ .

Remark 4.6 (Advantages of Algorithm 1). Algorithm 1 has two key structural advantages.

First, at each time step only two linear systems with the same SPD matrix  $L = I + \frac{\tau}{2}A$  need to be solved, independently of the unknown coefficient  $r^{n+\frac{1}{2}}$ . This allows the use of efficient iterative solvers (such as preconditioned conjugate gradients) with a fixed preconditioner, and, in the case of a fixed spatial grid, a single factorisation of L can be reused for all right-hand sides.

Second, the overdetermination condition is incorporated in a purely algebraic way: the midpoint identity (4.21) yields the closed formula (4.24), so that the inverse problem at each time level reduces to a scalar update for  $r^{n+\frac{1}{2}}$  followed by a

linear state update for  $U^{n+1}$ . No nonlinear iterations are required as long as the denominator in (4.24) remains bounded away from zero, which corresponds to a natural identifiability condition on the pair  $(f, \omega)$ .

### 5. Numerical Experiments

To validate the proposed algorithm and assess its accuracy and convergence properties, we present a set of numerical experiments. We consider a manufactured solution to the inverse problem (1.1)–(1.4), which allows for direct comparison against known ground truth. And to assess the robustness of these methods, we tested them using noisy integral data w(t) and its time derivative.

**Numerical example.** We consider two test problems on the domain  $Q = [0,1] \times [0,1]$ , with manufactured solutions and known exact data to assess the accuracy of the numerical reconstruction.

Example 1. The exact functions are chosen as

$$u(t,x) = (1+t^2+s\sin(t))\sin(\pi x) + ste^{-t}\sin(3\pi x), \qquad r(t) = 1+\frac{s}{2}(1+\cos(t)),$$
  
$$\omega(x) = \sin(\pi x), \quad w(t) = \frac{1}{2}(1+t^2+s\sin(t)),$$

and the function f(t,x) is calculated as follows:

$$f(t,x) = \frac{u_t(t,x) + (-\Delta)^s u(t,x)}{r(t)}.$$

**Example 2.** The data are defined as follows

$$u(t,x) = \cos(t)\sin(\pi x) + ste^{-t}\sin(2\pi x), r(t) = 1 + \sin(t),$$

$$\omega(x) = \begin{cases} 1, & x \in [0.4, 0.6], \\ 0, & \text{otherwise,} \end{cases}, w(t) = \frac{\sqrt{5} - 1}{2\pi}\cos t.$$

Figure 1 provides a graphical visualisation of the function  $\omega(x)$  for two test cases, highlighting its behaviour and structure across the spatial domain.

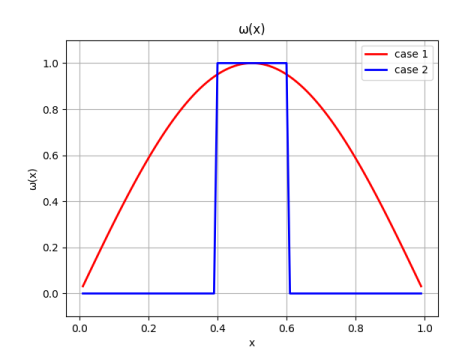


FIGURE 1. Graphical visualisation of  $\omega(x)$  for Test Example 1 and Example 2.

Figure 2 compares the analytical solution and the numerical results of Example 1 for u(t,x) and r(t) obtained using CN-Riesz approach on a uniform grid with N=M=100.

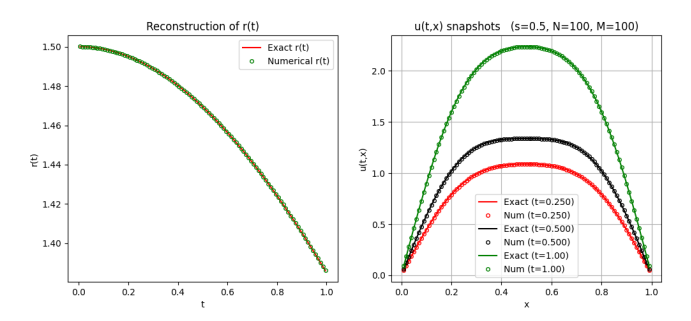


FIGURE 2. Analytical vs numerical solutions of r(t) and u(t,x) at T=1.

Figure 3 compares the analytical solution and the numerical results of Example 2 for u(t,x) and r(t) obtained using CNN-Riesz approach on a uniform grid with N=M=100.

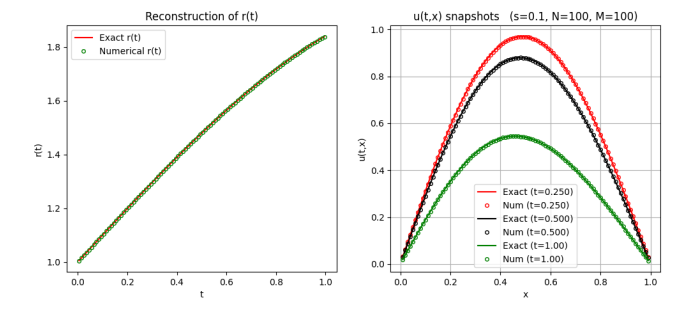


FIGURE 3. Analytical vs numerical solutions of r(t) and u(t,x) at T=1.

From Figures 2, 3, it is evident that our *CN-Riesz approach* achieves excellent accuracy in both state and coefficient reconstruction. Notably, it retains high fidelity even when the spatial step is coarser than the temporal step. Precision can be further improved with a stricter convergence tolerance in the iteration.

Figure 4 compares the numerical results of Example 1 for u(t, x) and r(t) for various values of s that is s := 0.1; 0.2; 0.3; 0.4; 0.5; 0.6; 0.7; 0.8; 0.9.

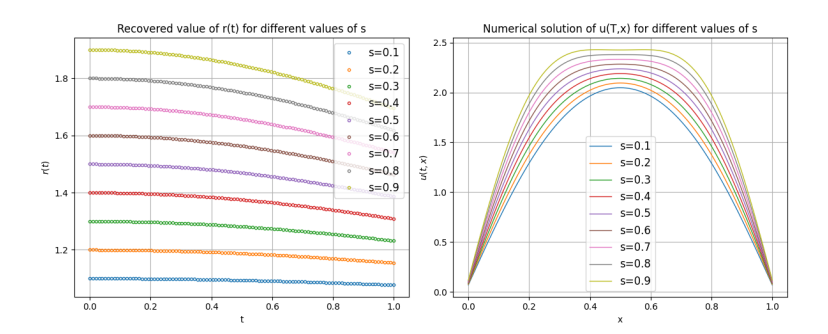


FIGURE 4. Numerical solutions of r(t) and u(t, x) at T = 1 for different values of s.

From this result, we see how strongly the value of s can influence the values of u(t,x) and r(t). From the left figure, it is clear that s can influence the coefficient r(t) more than the value of u(t,x).

Tables 1 and 2 report the accuracy and convergence behaviour of our CN-Riesz approach method.

Table 1. Calculated errors at varying  $\tau$  for fixed h=1/800, s=0.5

au	$L^{\infty}$ error in $u$	$L^2$ in $u$	$L^{\infty}$ error in $r$
-1/50	1.745e-05	1.244e-05	1.317e-04
1/100	4.362e-06	3.110e-06	3.327e-05
1/200	1.089e-06	7.767e-07	8.359e-06
1/400	2.685e-07	1.924e-07	2.095e-06
1/800	6.680e-08	4.762e-08	5.244e-07

Table 2. Calculated errors at varying h with  $\tau = h, s = 0.1$ 

h	$L^{\infty}$ error in $u$	$L^2$ in $u$	$L^{\infty}$ error in $r$
1/100	1.255e-06	9.256e-07	2.481e-05
1/200	3.078e-07	2.296e-07	6.230 e-06
1/400	7.561e-08	5.695e-08	1.561e-06
1/800	1.939e-08	1.413e-08	3.907e-07

**Discussion.** The numerical results demonstrate that the proposed CN-Riesz method achieves superior accuracy for both the state solution u(t, x) and the coefficient recovery r(t).

5.1. Sensitivity of the numerical methods to noisy data. To test our methods under realistic conditions, we conducted experiments in which both the overdetermination data w(t) and its time derivative were corrupted by additive noise. We defined

$$w^{\delta}(t) = w(t) + \delta \eta(t), \qquad \partial_t w^{\delta}(t) = \partial_t w(t) + \delta \xi(t),$$

with  $\delta \in \{0.01, 0.03, 0.05\}$  (corresponding to 1 %, 3 %, and 5 % noise levels) and  $\eta(t)$ ,  $\xi(t)$  as random perturbations simulating measurement errors. The noisy signals  $w^{\delta}(t)$  and  $\partial_t w^{\delta}(t)$  were then used in place of the exact values in the coefficient-recovery formula.

Testing the numerical algorithm on noisy data. The results are presented in Figures 5, where each plot compares the exact and numerically reconstructed values of r(t) under different noise levels.

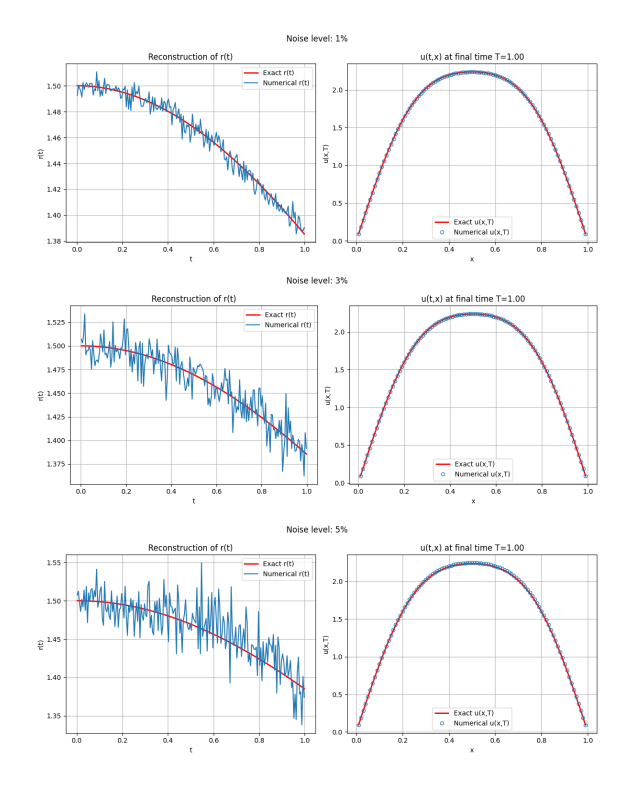


FIGURE 5. Left: Exact and numerically reconstructed r(t) under 1 %, 3 %, and 5 % noise in the overdetermination data. Right: heat distribution function u(t,x) showing the exact (red) and its numerical calculation, circled marker (blue).

The results demonstrate the ability of our numerical approach to efficiently handle noisy data, making it suitable for practical applications where accurate measurements are rarely available. From the figure 5, it is clear that our numerical approach remains stable even with 1%-5% noise and yields significantly smoother reconstructions.

#### 6. Conclusion

We developed a robust numerical framework for the inverse problem of timedependent coefficient recovery in fractional heat equations. The approach consisted of three main components: first, we established well-posedness of the forward problem via a priori estimates; second, we constructed a Crank–Nicolson discretization with proven stability and optimal convergence rates; and third, we validated the method through extensive numerical simulations that confirmed accurate reconstructions even under significant measurement noise. These results underscored the method's strong potential for practical applications.

#### Data availability

All data will be made available by the corresponding author upon reasonable request.

#### Funding

The research is financially supported by a grant from the Ministry of Science and Higher Education of the Republic of Kazakhstan (No. AP27508473), by the FWO Research Grant G083525N: Evolutionary partial differential equations with strong singularities, and by the Methusalem programme of the Ghent University Special Research Fund (BOF) (Grant number 01M01021)..

#### References

- [1] Deng W.H., Zhang Z.J., High Accuracy Algorithm for the Differential Equations Governing Anomalous Diffusion, World Scientific, Singapore (2019).
- [2] Applebaum D., Lévy Processes and Stochastic Calculus, Cambridge University Press, New York (2009).
- [3] Kwaśnicki M., Ten equivalent definitions of the fractional Laplace operator, Fract. Calc. Appl. Anal. 20 (1) (2017) 7–51. https://doi.org/10.1515/fca-2017-0002
- [4] Daoud M., Laamri E.H., Fractional Laplacians: a short survey, Discrete Contin. Dyn. Syst. Ser. S 15 (1) (2022) 95-116. https://doi.org/10.3934/dcdss.2021027
- [5] Valdinoci E., From the long jump random walk to the fractional Laplacian, Bol. Soc. Esp. Mat. Apl. 49 (2009) 33-44.
- [6] Vázquez J.L., The mathematical theories of diffusion: nonlinear and fractional diffusion, in: Bonforte M., Grillo G. (Eds.), Nonlocal and Nonlinear Diffusions and Interactions: New Methods and Directions, Lecture Notes in Mathematics, vol. 2186, Springer, Cham (2019).
- [7] Acosta G., Bersetche F.M., Bothagaray J.P., A short FE implementation for a 2D homogeneous Dirichlet problem of a fractional Laplacian, Comput. Math. Appl. 74 (2017) 784-816. https://doi.org/10.1016/j.camwa.2017.05.026
- [8] Raible S., Lévy processes in finance: theory, numerics, and empirical facts, Ph.D. thesis, Universität Freiburg (2000).
- [9] Mccay B.M., Narasimhan M.N.L., Theory of nonlocal electromagnetic fluids, Arch. Mech. 33 (1981) 365–384.
- [10] John H., Ginn T.R., Nonlocal dispersion in media with continuously evolving scales of heterogeneity, Transp. Porous Media 13 (1993) 123-138. https://doi.org/10.1007/BF00613273
- [11] Bouchaud J., Georges A., Anomalous diffusion in disordered media: statistical mechanisms, models and physical applications, Phys. Rep. 195 (4-5) (1990) 127-293. https://doi.org/ 10.1016/0370-1573(90)90099-N
- [12] Humphries N.E., Weimerskirch H., Queiroz N., Southall E., Sims D., Foraging success of biological Lévy flights recorded in situ, Proc. Natl. Acad. Sci. USA 109 (19) (2012) 7169– 7174. https://doi.org/10.1073/pnas.1121201109
- [13] Duo S., van Wyk H.W., Zhang Y., A novel and accurate finite difference method for the fractional Laplacian and the fractional Poisson problem, J. Comput. Phys. 355 (2018) 233– 252. https://doi.org/10.1016/j.jcp.2017.11.011
- [14] Duo S., Zhang Y., Accurate numerical methods for two and three-dimensional integral fractional Laplacian with applications, Comput. Methods Appl. Mech. Eng. 355 (2019) 639–662. https://doi.org/10.1016/j.cma.2019.06.016
- [15] Gu X., Sun H., Zhang Y., Zhao Y., Fast implicit difference schemes for time-space fractional diffusion equations with the integral fractional Laplacian, Math. Methods Appl. Sci. 44 (2021) 441-463. https://doi.org/10.1002/mma.6746

- [16] Han R., Wu S., A monotone discretization for integral fractional Laplacian on bounded Lipschitz domains: pointwise error estimates under Hölder regularity, SIAM J. Numer. Anal. 60 (2022) 3052–3077. https://doi.org/10.1137/21M1448239
- [17] Huang Y., Oberman A., Numerical methods for the fractional Laplacian: a finite difference-quadrature approach, SIAM J. Numer. Anal. 52 (6) (2014) 3056-3084. https://doi.org/10.1137/140954040
- [18] Huang W., Shen J., A grid-overlay finite difference method for the fractional Laplacian on arbitrary bounded domains, SIAM J. Sci. Comput. 46 (2024) A744-A769. https://doi.org/ 10.1137/23M1558562
- [19] Wu Y., Zhang Y., Highly accurate operator factorization methods for the integral fractional Laplacian and its generalization, Discrete Contin. Dyn. Syst. Ser. S 15 (2022) 851–876. https://doi.org/10.3934/dcdss.2022016
- [20] Yang H., Chen H., Yue X., Long G., High-order fractional central difference method for multidimensional integral fractional Laplacian and its applications, Commun. Nonlinear Sci. Numer. Simul. 145 (2025) 108711. https://doi.org/10.1016/j.cnsns.2025.108711
- [21] Acosta G., Borthagaray J.P., A fractional Laplace equation: regularity of solutions and finite element approximations, SIAM J. Numer. Anal. 55 (2017) 472-495. https://doi.org/10. 1137/15M1033952
- [22] Acosta G., Borthagaray J.P., Heuer N., Finite element approximations of the nonhomogeneous fractional Dirichlet problem, IMA J. Numer. Anal. 39 (2019) 1471–1501. https://doi.org/10.48550/arXiv.1709.06592
- [23] Chen H., Sheng C., Wang L., On explicit form of the FEM stiffness matrix for the integral fractional Laplacian on nonuniform meshes, Appl. Math. Lett. 113 (2021) 106864. https://doi.org/10.1016/j.aml.2020.106864
- [24] Sheng C., Wang L.L., Chen H., Li H., Fast implementation of FEM for integral fractional Laplacian on rectangular meshes, Commun. Comput. Phys. 36 (2024) 673-710. https://doi.org/10.4208/cicp.0A-2023-0011
- [25] Zhou J., Chen H., Finite element method on locally refined composite meshes for Dirichlet fractional Laplacian, J. Comput. Sci. 82 (2024) 102433. https://doi.org/10.1016/j.jocs. 2024.102433
- [26] Duo S., Zhang Y., Mass-conservative Fourier spectral methods for solving the fractional nonlinear Schrödinger equation, Comput. Math. Appl. 71 (2016) 2257-2271. https://doi. org/10.1016/j.camwa.2015.12.042
- [27] Hao Z., Li H., Zhang Z., Zhang Z., Sharp error estimates of a spectral Galerkin method for a diffusion-reaction equation with integral fractional Laplacian on a disk, Math. Comput. 90 (2021) 2107-2135. https://doi.org/10.1090/mcom/3645
- [28] Kirkpatrick K., Zhang Y., Fractional Schrödinger dynamics and decoherence, Phys. D: Non-linear Phenom. 332 (2016) 41–54. https://doi.org/10.1016/j.physd.2016.05.015
- [29] Prilepko A.I., Orlovsky D.G., Vasin I.A., Methods for Solving Inverse Problems in Mathematical Physics, vol. 231, Marcel Dekker, Inc., New York, 2000. https://doi.org/10.1201/9781482292985
- [30] Grimmonprez M., Marin L., Van Bockstal K., The reconstruction of a solely time-dependent load in a simply supported non-homogeneous Euler-Bernoulli beam, Appl. Math. Model. 79 (2020) 914-933. https://doi.org/10.1016/j.apm.2019.10.066
- [31] Van Bockstal K., Marin L., Finite element method for the reconstruction of a time-dependent heat source in isotropic thermoelasticity systems of type-III, Z. Angew. Math. Phys. 73 (2022), 113, https://doi.org/10.1007/s00033-022-01750-8.
- [32] Hendy A.S., Van Bockstal K., A solely time-dependent source reconstruction in a multiterm time-fractional order diffusion equation with non-smooth solutions, Numer. Algorithms 90 (2022) 809–832. https://doi.org/10.1007/s11075-021-01210-w
- [33] Hendy A.S., Van Bockstal K., On a reconstruction of a solely time-dependent source in a time-fractional diffusion equation with non-smooth solutions, J. Sci. Comput. 90 (2022) 33. https://doi.org/10.1007/s10915-021-01704-8
- [34] Durdiev D., Rahmonov A., Global solvability of inverse coefficient problem for one fractional diffusion equation with initial non-local and integral overdetermination conditions, *Fract. Calc. Appl. Anal.* **28** (2025) 117–145. https://doi.org/10.1007/s13540-024-00367-0

- [35] Helin T., Lassas M., Ylinen L., Zhang Z., Inverse problems for heat equation and space-time fractional diffusion equation with one measurement, J. Differ. Equ. 269 (9) (2020) 7498-7528. https://doi.org/10.1016/j.jde.2020.05.022
- [36] Ghosh T., Rüland A., Salo M., Uhlmann G., Uniqueness and reconstruction for the fractional Calderón problem with a single measurement, J. Funct. Anal. 279 (1) (2020) 108505. https://doi.org/10.1016/j.jfa.2020.108505
- [37] Guerngar N., Nane E., Tinaztepe R., et al., Simultaneous inversion for the fractional exponents in the space-time fractional diffusion equation  $\partial_t^{\beta} u = -(-\Delta)^{\alpha/2} u (-\Delta)^{\gamma/2} u$ , Fract. Calc. Appl. Anal. **24** (2021) 818–847. https://doi.org/10.1515/fca-2021-0035
- [38] Li L., On inverse problems for uncoupled space-time fractional operators involving timedependent coefficients, Inverse Probl. Imaging 17 (4) (2023) 890-906. https://doi.org/10. 3934/ipi.2023008
- [39] Kow P.Z., Wang J.N., Inverse problems for some fractional equations with general nonlinearity, Res. Math. Sci. 10 (2023) 45. https://doi.org/10.1007/s40687-023-00409-8
- [40] Kow P.Z., Ma S., Sahoo S.K., An inverse problem for semilinear equations involving the fractional Laplacian, Inverse Probl. 39 (2023) 095006. https://doi.org/10.1088/1361-6420/ ace9f4
- [41] Mamanazarov A., Suragan D., Inverse coefficient problems for the heat equation with fractional Laplacian, Fract. Calc. Appl. Anal. 28 (2025) 1324–1352. https://doi.org/10.1007/ s13540-025-00414-4
- [42] Fujishiro K., Kian Y., Determination of time dependent factors of coefficients in fractional diffusion equations, Math. Control Relat. Fields 6 (2) (2016) 251–269. https://hal.science/ hal-01101556v1
- [43] Hazanee A., Ismailov M.I., Lesnic D., Kerimov N.B., An inverse time-dependent source problem for the heat equation, Appl. Numer. Math. 69 (2013) 13-33. https://doi.org/10.1016/ j.apnum.2013.02.004
- [44] Hazanee A., Lesnic D., Determination of a time-dependent coefficient in the bioheat equation, Int. J. Mech. Sci. 88 (2014) 259–266. https://doi.org/10.1016/j.ijmecsci.2014.05.017
- [45] Ismailov M., Ozawa T., Suragan D., Inverse problems of identifying the time-dependent source coefficient for subelliptic heat equations, Inverse Probl. Imaging 18 (4) (2024) 813– 823. https://doi.org/10.3934/ipi.2023056
- [46] Tian W., Zhou H., and Deng W., A class of second order difference approximations for solving space fractional diffusion equations, Mathematics of Computation, 84(294) (2015) 1703-1727. https://doi.org/10.1090/S0025-5718-2015-02917-2
- [47] Brezis H., Functional Analysis, Sobolev Spaces and Partial Differential Equations, Springer, New York (2010).
- [48] Evans L.C., Partial Differential Equations, 2nd ed., Graduate Studies in Mathematics, vol. 19, American Mathematical Society, Providence, RI (2010).
- [49] Zeidler E., Nonlinear Functional Analysis and its Applications I: Fixed-Point Theorems, Springer-Verlag, New York (1986).

#### Arshyn Altybay:

INSTITUTE OF MATHEMATICS AND MATHEMATICAL MODELING,

125 Pushkin Str., 050010 Almaty, Kazakhstan

AN

Department of Mathematics: Analysis, Logic and Discrete Mathematics, Ghent University, Krijgslaan 281, Building S8, B 9000 Ghent, Belgium

E-mail address arshyn.altybay@ugent.be, arshyn.altybay@gmail.com

#### NIYAZ TOKMAGAMBETOV:

AL-FARABI KAZAKH NATIONAL UNIVERSITY

71 AL-FARABI AVE., 050040 ALMATY, KAZAKHSTAN

AND

Institute of Mathematics and Mathematical Modeling

125 Pushkin str., 050010 Almaty, Kazakhstan

E-mail address: tokmagambetov@math.kz

#### Gulzat Nalzhupbayeva:

al-Farabi Kazakh National University

71 al—Farabi ave., 050040 Almaty, Kazakhstan and Institute of Mathematics and Mathematical Modeling 125 Pushkin str., 050010 Almaty, Kazakhstan  $E\text{-}mail\ address:}$  Gulzat Nalzhupbayeva